

## Evidence for Two Separate Energy Gaps in Underdoped High-Temperature Cuprate Superconductors from Broadband Infrared Ellipsometry

Li Yu,<sup>1,2</sup> D. Munzar,<sup>3</sup> A. V. Boris,<sup>2</sup> P. Jordanov,<sup>2</sup> J. Chaloupka,<sup>3</sup> Th. Wolf,<sup>4</sup> C. T. Lin,<sup>2</sup> B. Keimer,<sup>2</sup> and C. Bernhard<sup>1,2</sup>

<sup>1</sup>Department of Physics and Fribourg Center for Nanomaterials, University of Fribourg, Chemin du Musée 3, CH-1700 Fribourg CH, Switzerland

<sup>2</sup>Max-Planck-Institute for Solid State Research, Heisenbergstrasse 1, D-70569 Stuttgart, Germany

<sup>3</sup>Institute of Condensed Matter Physics, Faculty of Science, Masaryk University, Kotlářská 2, CZ-61137 Brno, Czech Republic

<sup>4</sup>Forschungszentrum Karlsruhe, IFP, D-76021 Karlsruhe, Germany

We present broadband infrared ellipsometry measurements of the  $c$ -axis conductivity of underdoped  $\text{RBa}_2\text{Cu}_3\text{O}_{7-\delta}$  ( $R = \text{Y}, \text{Nd}, \text{and La}$ ) single crystals. Our data show that separate energy scales are underlying the redistributions of spectral weight due to the normal state pseudogap and the superconducting gap. Furthermore, they provide evidence that these gaps do not share the same electronic states and do not merge on the overdoped side. Accordingly, our data are suggestive of a two gap scenario with a pseudogap that is likely extrinsic with respect to superconductivity.

PACS numbers: 74.72.-h, 74.25.Gz, 78.20.-e, 78.30.-j

It is now widely recognized that the anomalous normal state properties of the high-temperature cuprate superconductors may hold the key for understanding the superconducting (SC) pairing mechanism. The most challenging feature is the pseudogap (PG), which prevails in the underdoped regime of the dome-shaped phase diagram of the SC transition temperature  $T_c$  versus hole doping  $p$  [1,2]. The PG gives rise to a depletion of the low-energy electronic excitations already in the normal state that has been identified with techniques like specific heat [3], angle-resolved photoemission spectroscopy (ARPES) [4,5],  $c$ -axis tunneling [6], and also by far infrared spectroscopy [7–9]. While these have established important aspects, like its strong  $k$ -space anisotropy [4,5] or its rapid rise on the underdoped side [4,9], the origin of the PG and, in particular, the question of whether it is intrinsic or extrinsic with respect to superconductivity remains heavily debated [2,3,5,10,11]. Prominent intrinsic theories are the phase fluctuation model where the PG corresponds to a SC state lacking macroscopic phase coherence [12], precursor pairing models where the pair formation occurs at much higher temperature ( $T$ ) than the condensation [13], and the resonating valence bond theory [14]. The extrinsic models include numerous conventional and exotic spin- or charge-density wave states [15]. One of the major obstacles in identifying the relevant theory is the lack of a clear spectroscopic distinction between the PG and the SC gap.

In this Letter we present broadband infrared (70–4000  $\text{cm}^{-1}$ ) ellipsometry measurements of the  $c$ -axis conductivity of underdoped  $\text{RBa}_2\text{Cu}_3\text{O}_{7-\delta}$  ( $R = \text{Y}, \text{Nd}, \text{La}$ ) single crystals which shed new light on this issue.

The high quality crystals were flux grown in Y-stabilized zirconium crucibles under reduced oxygen atmosphere to avoid substitution of  $R$  ions on the Ba site [16]. The oxygen content  $\delta$  and the consequent hole doping  $p$  were adjusted by annealing in flowing  $\text{O}_2$  and rapid quenching. The

quoted  $T_c(\Delta T_c)$  values correspond to the midpoint (10% to 90% width) of the diamagnetic transition from SQUID magnetometry. The  $p$  values were deduced with the empirical relationship  $p = 0.16 \pm \sqrt{\frac{1-T_c/T_{c,\text{max}}}{82.6}}$  [2], with  $T_{c,\text{max}} = 92.5, 96, \text{ and } 98$  K for Y, Nd, and La [17]. The  $\delta$  values for a fixed doping level decrease with increasing size of the  $R$  ion [17]; i.e., for  $p \approx 0.12$  the annealing  $T$  (in  $\text{O}_2$ ),  $\delta$ , and  $T_c$  values are 570 °C, 0.2, 82(1) K for  $\text{YBa}_2\text{Cu}_3\text{O}_{7-\delta}$  (Y-123), 440 °C, 0.1, 85(2) K for  $\text{NdBa}_2\text{Cu}_3\text{O}_{7-\delta}$  (Nd-123), and 310 °C, 0, 87(2) K for  $\text{LaBa}_2\text{Cu}_3\text{O}_{7-\delta}$  (La-123), respectively.

We used a home-built ellipsometer attached to a Bruker fast-Fourier spectrometer at the infrared beam line of the ANKA synchrotron at Forschungszentrum Karlsruhe D, Germany, at 70–700  $\text{cm}^{-1}$  and a similar lab-based setup at 400–4000  $\text{cm}^{-1}$  [18]. All spectra have been corrected for anisotropy effects [18,19]. Ellipsometry directly measures the complex dielectric function,  $\tilde{\epsilon} = \epsilon_1 + i\epsilon_2$ , and the related optical conductivity  $\tilde{\sigma}(\omega) = \frac{i\omega}{4\pi}[1 - \tilde{\epsilon}(\omega)]$ , without a need for Kramers-Kronig analysis [19]. Furthermore, it is a self-normalizing technique that is very accurate and reproducible.

Figure 1 summarizes our  $c$ -axis conductivity,  $\sigma_{1c}(\omega)$ , data for underdoped  $\text{NdBa}_2\text{Cu}_3\text{O}_{6.9}$  ( $p \approx 0.12$ ). Representative spectra in the PG and SC states are shown in Figs. 1(a) and 1(b), respectively, the  $T$ -difference spectra,  $\Delta\sigma_{1c} = \sigma_{1c}(T) - \sigma_{1c}(300 \text{ K})$ , are given in Fig. 1(c). The  $T$  dependence of the spectral weight,  $(\text{SW})_\alpha^\beta = \int_\alpha^\beta \sigma_{1c}(\omega) d\omega$ , for representative limits is given in Figs. 1(d)–1(f). First, we focus on the PG which manifests itself as a suppression of  $\sigma_{1c}(\omega)$  below the crossing point between the 240 K and the 90 K spectra at  $\omega_{\text{PG}} \approx 700 \text{ cm}^{-1}$ . Its onset temperature of  $T^* \approx 220$  K is readily deduced from the  $T$  dependence of  $(\text{SW})_{0^+}^{800}$  in Fig. 1(d). In addition to these established features [1,7–9,20], our data

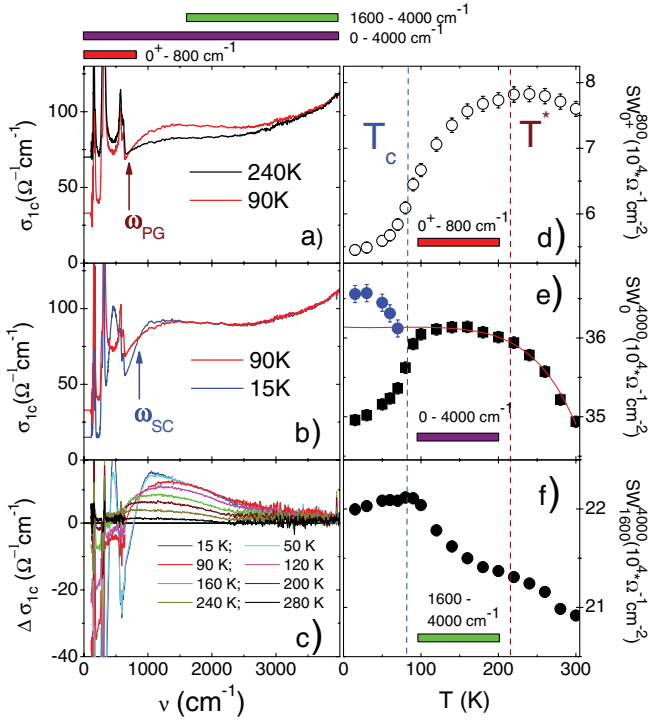


FIG. 1 (color). C-axis conductivity of underdoped  $\text{NdBa}_2\text{Cu}_3\text{O}_{6.9}$ . Shown are representative spectra for (a) the PG state, (b) the SC state, and (c) the  $T$  difference,  $\Delta\sigma_{1c} = \sigma_{1c}(T) - \sigma_{1c}(300 \text{ K})$ . Brown (blue) arrows mark the crossing points at  $\omega_{\text{PG}}$  ( $\omega_{\text{SC}}$ ). The  $T$  dependence of the spectral weight,  $(\text{SW})_{\alpha}^{\beta} = \int_{\alpha}^{\beta} \sigma_{1c}(\omega) d\omega$ , is shown for (d)  $\alpha = 0$  and  $\beta = 800 \text{ cm}^{-1}$  (regular part), (e)  $\alpha = 0$  and  $\beta = 4000 \text{ cm}^{-1}$  [black squares show the regular part, while blue circles include the SC delta function  $(\text{SW})^{\delta}$ ], and (f)  $\alpha = 1600$  and  $\beta = 4000 \text{ cm}^{-1}$ . Vertical bars show the statistical errors. The red line in (e) shows a fit to the normal state data with the function  $\text{SW}(T) = (\text{SW})_0 [1 - (T/T_c)^{\beta}]$ .

reveal the energy scale that governs the PG-related SW redistribution. Figures 1(a) and 1(c) show that the SW loss with decreasing  $T$  due to the decrease of  $\sigma_{1c}(\omega < \omega_{\text{PG}})$  is accompanied by a SW gain in the midinfrared (MIR) region due to the development of a broad band that extends from the gap edge to about  $3500 \text{ cm}^{-1}$ . The balance between the SW decrease at  $\omega < \omega_{\text{PG}}$  and the SW gain at  $\omega_{\text{PG}} < \omega < 4000 \text{ cm}^{-1}$  is evident from the smooth evolution of  $(\text{SW})_{0+}^{4000}$  in Fig. 1(e), which, unlike  $(\text{SW})_{0+}^{800}$  in Fig. 1(d), does not decrease below  $T^*$ . The continuous increase of  $(\text{SW})_{0+}^{4000}$  with decreasing  $T$  at  $T > T_c$  is not related to the PG phenomenon because it is most prominent above  $T^*$ , it involves an overall SW gain at  $\omega < 4000 \text{ cm}^{-1}$  [see Fig. 1(c)], and it even occurs in strongly overdoped samples where the PG is absent (not shown) and also for the in-plane response [21]. Returning to the PG phenomenon, our data establish that the underlying energy scale is less than  $4000 \text{ cm}^{-1}$  (or  $0.5 \text{ eV}$ ). Notably, the spectral shape of the related changes in  $\sigma_{1c}(\omega)$  resembles the one of some BCS-type spin- or charge-density wave

systems [22]. The SW is redistributed here from the region below the gap edge at  $2\Delta_{\text{DW}}/\hbar$ , where  $\Delta_{\text{DW}}$  is the density wave gap, to a broad band that extends from the gap edge to about  $10\Delta_{\text{DW}}$ . However, the  $T$  dependence of the PG magnitude is not conventional (BCS-like) since the PG does not seem to close at  $T^*$  but merely fills in with thermally excited states.

Another important question is what impact the SC transition has on the PG-related SW redistribution, i.e., on the MIR band. For this we focus on the data at  $\omega > 1600 \text{ cm}^{-1}$  which are not affected by the narrower, superconductivity-induced band near  $1000 \text{ cm}^{-1}$  that is discussed below. In the first place, Figs. 1(b) and 1(c) show that  $\sigma_{1c}(\omega > 1600 \text{ cm}^{-1})$ , and thus the broad MIR band hardly changes below  $T_c$ . However, a closer inspection of the  $T$  dependence of  $(\text{SW})_{1600}^{4000}$  in Fig. 1(f) reveals a significant impact of the SC transition on the MIR band. Its increasingly rapid growth below  $T^*$  [as compared to the smooth evolution of  $(\text{SW})_{0+}^{4000}$  in Fig. 1(e)] is suddenly interrupted at  $T_c$  below which it saturates. We note that the same trend is observed for a series of underdoped Y-123 crystals (not shown). Interestingly, this unusual behavior compares well with a recent ARPES study which reveals a distinct PG that first appears in the antinodal region of the Brillouin zone (near the X point) and expands with decreasing  $T$  along the Fermi surface. This expansion appears to be intersected by the SC gap which develops below  $T_c$  on the remaining parts of the Fermi surface [5]. These observations suggest that the PG and SC gaps are separate and likely even competitive phenomena that do not share the same electronic states. Certainly, our data challenge phase fluctuation models of the PG. Here one would naively expect that, once the phase fluctuations diminish below  $T_c$ , a significant part of the PG-related SW should be transferred back to low energies and join the SC condensate (see [23]). Figures 1(b) and 1(c) establish that this is not the case. Therefore, while precursor SC fluctuations are well established [24], it seems that they are a consequence of the PG (rather than its cause) which depletes the low-energy SW that is available for superconductivity. We note that the minor decrease of  $(\text{SW})_{0+}^{4000}$  below about  $120 \text{ K}$  may be a corresponding signature.

Our data also confirm previous reports that the SW transfer in the SC state involves an anomalously high energy scale [25]. This can be seen in Fig. 1(e) from the anomalous increase below  $T_c$  of  $(\text{SW})_0^{4000}$  (blue circles) which includes the SW of the SC delta function,  $(\text{SW})^{\delta}$ .  $(\text{SW})^{\delta}$  is deduced by fitting a Drude-Lorentz model to the complex dielectric function. The comparison with the normal state trend (red line) as estimated by a power law fit suggests that about 20% of  $(\text{SW})^{\delta}$  originates from above  $4000 \text{ cm}^{-1}$ . Notably, our data highlight that this anomalous contribution to  $(\text{SW})^{\delta}$  does not arise from the PG-related MIR bands; i.e., the SW redistributions in the PG and the SC states involve different energy scales.

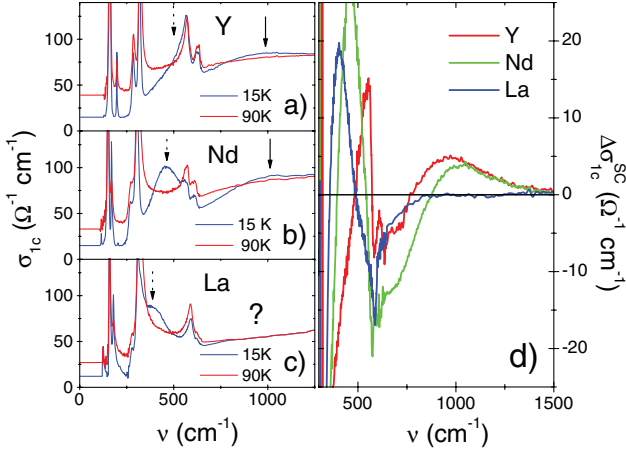


FIG. 2 (color). (a)–(c)  $C$ -axis conductivity of  $R$ -123 ( $R = \text{Y, Nd, and La}$ ) with  $p \approx 0.12$ . Dotted (solid) arrows mark the transverse Josephson plasma mode (the mode near  $1000 \text{ cm}^{-1}$ ). (d) Difference spectra,  $\Delta\sigma_{1c} = \sigma_{1c}(10 \text{ K}) - \sigma_{1c}(90 \text{ K})$ .

Next we discuss the  $p$  dependence of the gaps. Here we use the frequencies  $\omega_{\text{PG}}$  and  $\omega_{\text{SC}}$  of the crossing points in the  $\sigma_{1c}$  spectra as the characteristic ones to be compared to the gap magnitudes,  $2\Delta_{\text{PG}}$  and  $2\Delta_{\text{SC}}$ . The relation  $\hbar\omega_{\text{PG}} \approx 2\Delta_{\text{PG}}$  can indeed be justified with model calculations of the type presented in Ref. [9] by using fits of the quasiparticle spectral functions of Ref. [26] (not shown). The justification of the relation  $\hbar\omega_{\text{SC}} \approx 2\Delta_{\text{SC}}$  involves the  $1000 \text{ cm}^{-1}$  mode which occurs right above  $\omega_{\text{SC}}$  in the spectra below  $T_c$ . In the first place, it may correspond to an interband (bonding-antibonding) pair-breaking peak whose coherence factor decreases with decreasing bilayer coupling [27]. This interpretation is supported by our data for underdoped  $R$ -123 crystals in Fig. 2. The mode intensity exhibits a clear decrease with increasing radius of the rare earth ion of 1.019, 1.109, and  $1.16 \text{ \AA}$  for  $\text{Y}^{3+}$ ,  $\text{Nd}^{3+}$ , and  $\text{La}^{3+}$  [17]. A corresponding decrease of the bilayer coupling is confirmed by recent ARPES data [28] and also by the redshift of the so-called transverse Josephson plasma resonance mode [29] near  $500 \text{ cm}^{-1}$ . Alternatively, the  $1000 \text{ cm}^{-1}$  mode may have the same origin as the maximum of the in-plane SC spectra near  $1000 \text{ cm}^{-1}$  which has been attributed to final states involving two Bogolyubov quasiparticles and a bosonic mode (for a review see Ref. [8]). According to both interpretations, the mode is located just a few tens of meV above  $2\Delta_{\text{SC}}$ , thus yielding  $\hbar\omega_{\text{SC}} \approx 2\Delta_{\text{SC}}$ . While this procedure may not be sufficient for precise estimates of the gap magnitudes, it likely provides a reasonable and consistent means of examining the changes in gap values as a function of doping. Figure 3 displays the  $p$  dependence of  $\omega_{\text{PG}}/2$  and  $\omega_{\text{SC}}/2$  for a series of underdoped Y-123 crystals. For comparison we also show the gap values as obtained by recent APRES studies [5], which agree rather well. It is evident that  $\omega_{\text{PG}}$  exhibits a considerably stronger variation than  $\omega_{\text{SC}}$ , which remains almost constant on the under-

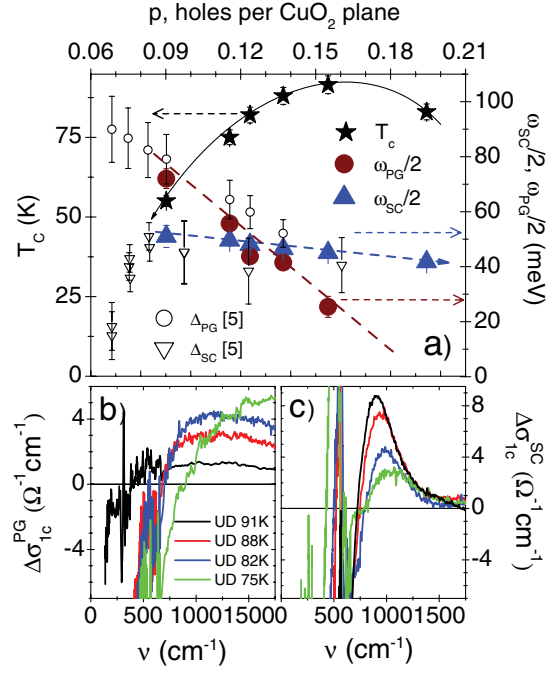


FIG. 3 (color). (a) Phase diagram of Y-123 giving the doping dependence of  $T_c$  (black stars),  $\omega_{\text{PG}}/2$  (brown circles), and  $\omega_{\text{SC}}/2$  (blue triangles). Open symbols show the corresponding gap values,  $\Delta_{\text{PG}}$  and  $\Delta_{\text{SC}}$ , from Ref. [5]. The dashed brown (blue) line shows a linear extrapolation of  $\omega_{\text{PG}}/2$  ( $\omega_{\text{SC}}/2$ ). (b),(c) Difference spectra,  $\Delta\sigma_{1c}^{\text{PG}} = \sigma_{1c}(T \approx T_c) - \sigma_{1c}(T \approx T^*)$  and  $\Delta\sigma_{1c}^{\text{SC}} = \sigma_{1c}(10 \text{ K}) - \sigma_{1c}(T \approx T_c)$ , from which  $\omega_{\text{PG}}$  and  $\omega_{\text{SC}}$  were deduced. For clarity we removed sharp features due to  $T$ -dependent shifts of some phonon modes.

doped side. The latter behavior, which may seem at variance with the apparent  $T_c$  decrease, is compatible with recent Nernst effect measurements [24] which yield a nearly constant onset temperature of the local SC pairing (except for  $p < 0.1$ ). Towards the overdoped side, we cannot follow the evolution of  $\omega_{\text{PG}}$  beyond optimum doping where  $T^* \leq T_c$ . Nevertheless, a linear extrapolation suggests that the PG vanishes around  $p_{\text{crit}} \approx 0.19\text{--}0.2$  as previously reported [2,20]. There may be some uncertainty about the exact value of  $\omega_{\text{PG}}$  at  $p = 0.15$  where it falls well in the range of the phonon modes. Nevertheless, we emphasize that in Fig. 3(b)  $\Delta\sigma_{1c}^{\text{PG}}$  in the PG state is clearly positive at frequencies much below the zero crossing of  $\Delta\sigma_{1c}^{\text{SC}}$  in the SC state in Fig. 3(c), which suggests that these gaps must be significantly different. This finding is incompatible with intrinsic models where  $\omega_{\text{PG}}$  and  $\omega_{\text{SC}}$  should merge on the overdoped side. Another interesting aspect is the observation of  $\omega_{\text{PG}} > \omega_{\text{SC}}$  at  $p < 0.12$  which suggests that the two gaps do not simply add to the spectroscopic gap, i.e., that they do not share the same electronic states. This observation again agrees well with the ARPES data of Ref. [5] which suggest that the gaps are separated in  $k$  space. A striking example of this behavior is given in Fig. 4(a), which shows the data for La-123. Here the superconductivity-induced mode around  $1000 \text{ cm}^{-1}$  is ab-

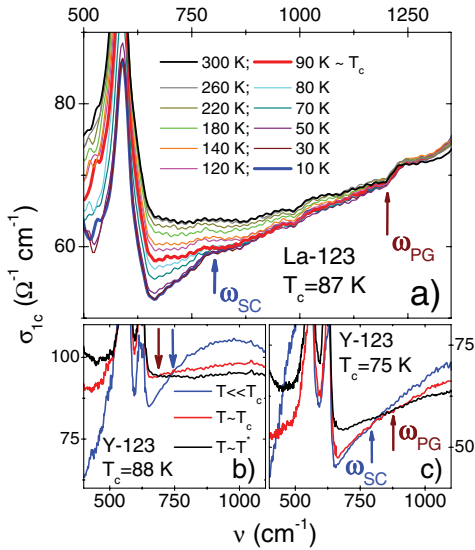


FIG. 4 (color). (a)  $C$ -axis conductivity spectra of  $\text{LaBa}_2\text{Cu}_3\text{O}_7$  showing the two separate crossing points at  $\omega_{\text{PG}}$  and  $\omega_{\text{SC}}$  as marked by brown and blue arrows. (b),(c) Conductivity spectra showing the corresponding crossing points at  $\omega_{\text{PG}}$  and  $\omega_{\text{SC}}$  for Y-123 with  $T_c = 88$  and  $75$  K.

sent, and the SC gap can be clearly associated with the shoulderlike feature at  $\omega_{\text{SC}} \approx 800 \text{ cm}^{-1}$  [30] which compares well with  $\omega_{\text{SC}} \approx 780 \text{ cm}^{-1}$  and  $860 \text{ cm}^{-1}$  in Y-123 and Nd-123. The value of  $\omega_{\text{PG}} \approx 1200 \text{ cm}^{-1}$  is significantly higher here allowing for a clear spectroscopic distinction between the two gaps. It remains to be explored whether this PG enhancement reflects a strong influence of the bilayer coupling or of structural disorder that may be caused by a partial substitution of La on the Ba site. Finally, Figs. 4(b) and 4(c) show corresponding spectra for underdoped Y-123 with  $T_c = 88$  and  $75$  K which detail the different crossing points at  $\omega_{\text{PG}}$  and  $\omega_{\text{SC}}$  and show that they exchange their relative positions as a function of doping (see also Fig. 3).

In conclusion, we presented broadband ellipsometry data which provide a clear spectroscopic distinction between the normal state pseudogap and the superconducting gap. They establish that the respective spectral weight redistributions involve different energy scales. In particular, the PG-related shift of spectral weight from low energies to a broad MIR band becomes arrested but not reversed in the SC state. Furthermore, the magnitude of the PG decreases much faster with increasing doping than the one of the SC gap, and the PG seems to disappear much earlier at  $p \sim 0.19$ . Our data thus support a two gap scenario with a PG that depletes the density of states available for superconductivity.

We acknowledge funding by the Schweizerische Nationalfonds, SNF (200021-111690), the Deutsche

Forschungsgemeinschaft, DFG (BE2684/1 in FOR538), and the Ministry of Education of the CR (MSM0021622410). We thank Y. L. Mathis for his support at ANKA.

- [1] T. Timusk and B. Statt, Rep. Prog. Phys. **62**, 61 (1999).
- [2] J. L. Tallon and J. W. Loram, Physica (Amsterdam) **349C**, 53 (2001).
- [3] J. W. Loram, K. A. Mirza, J. R. Cooper, and W. Y. Liang, Phys. Rev. Lett. **71**, 1740 (1993).
- [4] A. G. Loeser *et al.*, Science **273**, 325 (1996).
- [5] K. Tanaka *et al.*, Science **314**, 1910 (2006).
- [6] V. M. Krasnov, A. Yurgens, D. Winkler, P. Delsing, and T. Claeson, Phys. Rev. Lett. **84**, 5860 (2000).
- [7] C. C. Homes, T. Timusk, R. Liang, D. A. Bonn, and W. N. Hardy, Phys. Rev. Lett. **71**, 1645 (1993).
- [8] D. N. Basov and T. Timusk, Rev. Mod. Phys. **77**, 721 (2005).
- [9] C. Bernhard *et al.*, Phys. Rev. B **59**, R6631 (1999); Phys. Rev. Lett. **80**, 1762 (1998).
- [10] M. Kugler, O. Fischer, C. Renner, S. Ono, and Y. Ando, Phys. Rev. Lett. **86**, 4911 (2001).
- [11] N. Miyakawa, Physica (Amsterdam) **364C**, 475 (2001).
- [12] V. J. Emery and S. A. Kivelson, Nature (London) **374**, 434 (1995).
- [13] I. Kosztin, Q. Chen, Y. J. Kao, and K. Levin, Phys. Rev. B **61**, 11 662 (2000).
- [14] P. W. Anderson *et al.*, J. Phys. Condens. Matter **16**, R755 (2004).
- [15] A. V. Chubukov and J. Schmalian, Phys. Rev. B **57**, R11085 (1998); C. M. Varma, Phys. Rev. Lett. **83**, 3538 (1999).
- [16] S. I. Schlachter *et al.*, Int. J. Mod. Phys. B **14**, 3673 (2000).
- [17] G. V. M. Williams and J. L. Tallon, Physica (Amsterdam) **258C**, 41 (1996).
- [18] C. Bernhard, J. Humlicek, and B. Keimer, Thin Solid Films **455–456**, 143 (2004).
- [19] R. M. A. Azzam and N. H. Bashara, *Ellipsometry and Polarized Light* (North-Holland, Amsterdam, 1977).
- [20] A. V. Pimenov *et al.*, Phys. Rev. Lett. **94**, 227003 (2005).
- [21] M. Ortolani, P. Calvani, and S. Lupi, Phys. Rev. Lett. **94**, 067002 (2005).
- [22] M. Dressel and G. Grüner, *Electrodynamics of Solids* (Cambridge University Press, Cambridge, England, 2002).
- [23] L. B. Ioffe and A. J. Millis, Phys. Rev. B **61**, 9077 (2000).
- [24] Y. Wang *et al.*, Phys. Rev. Lett. **95**, 247002 (2005).
- [25] D. N. Basov *et al.*, Science **283**, 49 (1999).
- [26] M. R. Norman, M. Randeria, H. Ding, and J. C. Campuzano, Phys. Rev. B **57**, R11093 (1998).
- [27] D. Munzar, J. Phys. Chem. Solids **67**, 308 (2006).
- [28] S. Borisenko (private communication).
- [29] D. Munzar *et al.*, Solid State Commun. **112**, 365 (1999).
- [30] P. J. Hirschfeld, S. M. Quinlan, and D. J. Scalapino, Phys. Rev. B **55**, 12 742 (1997).